INCORPORATION OF BIGUANIDE COMPOUNDS INTO POLY(GL)-*b*-POLY(GL-*co*-TMC-*co*-CL)-*b*-POLY(GL) MONOFILAMENT SURGICAL SUTURES

Yolanda Márquez[1,2], Tània Cabral,[1] Alice Lorenzetti,[1]

Lourdes Franco[1], Pau Turon[2], Luís J. del Valle[1], Jordi Puiggalí[1*]

[1]Departament d'Enginyeria Química, Universitat Politècnica de Catalunya, Av. Diagonal 647, Barcelona E-08028, SPAIN

[2]B. Braun Surgical S.A., Carretera de Terrasa 121, Rubí (Barcelona), 08191, SPAIN

Correspondence to: **J. Puiggalí (Phone: 34-934015649, E-mail: Jordi.Puiggali@upc.edu)**

ABSTRACT

A new biodegradable coating was developed for bioabsorbable monofilament sutures. Specifically, a random copolymer having 35 wt-% and 65 wt-% of lactide and trimethylene carbonate units showed appropriate flexibility, stickiness and degradation rate, as well as capability to produce a complete and uniform coating. Monofilament sutures of polyglycolide-*b*-poly(glycolide-*co*-trimethylene carbonate-*co*-ε-caprolactone)-*b*-polyglycolide were loaded with chlorhexidine (CHX) and poly(hexamethylene biguanide) (PHMB) to explore the possibility to achieve antimicrobial activity without adverse cytotoxic effects. To this end, two processes based on single drug adsorption onto the suture surface and incorporation into the coating copolymer were used and subsequently evaluated. Although the second process could be considered more complex, clear benefits were observed in terms of drug loading efficiency, antimicrobial effect and even lack of cytotoxicity. In general, drugs could be loaded in an amount leading to a clear bacteriostatic effect for both Gram-negative and Gram-positive bacteria without causing significant cytotoxicity. Release profiles of PHMB and CHX were clearly different. Specifically, adsorption of the drug onto the fiber surface which prevented complete release was detected for PHMB. This polymer had advantages derived from its high molecular size, which hindered penetration into cells, thus resulting in lower cytotoxicity. Furthermore, bacterial growth kinetics measurements and bacterial adhesion assays showed greater effectiveness of this polymer.

Keywords: Monofilament sutures, chlorhexidine, poly(hexamethylene biguanide), antibacterial agent, polymer coating, drug release, cytotoxicity.

INTRODUCTION

Adhesion and proliferation of bacteria on the surface of materials are responsible for severe health problems. Microorganisms can survive on appropriate materials for long periods of time, especially in hospital environments, developing biofilms that could be involved in most chronic infections [1,2], hence the current demand of bacteriostatic, antiseptic and bactericidal agents to prevent bacterial survival and biofilm formation [3-5]. Today, 23% of surgical site infections [6] are caused by Gram-positive *Staphylococcus aureus* bacteria. Specifically, its drug-resistant strain becomes highly dangerous [7] since it could lead to patient mortality and high costs for society [8].

Typical bactericidal agents such as triclosan (TCS), chlorhexidine (CHX) and poly(hexamethylene biguanide) (PHMB) [9] have been employed to prevent bacterial infection. However, other natural agents like bacteriophages [10] can be considered, as well as industrial and clinical agents such as silver [11], quaternary ammonium groups [12], hydantoin compounds [13], and tetracycline antibiotics [14].

CHX (1,1′-hexamethylene-bis-5-(4-chlorophenyl)biguanide) (Figure 1) has a high activity towards microorganisms [15] as a consequence of the presence of secondary amines that can be protonated, and therefore positively charged under normal pH conditions [16]. Thus, CHX affects the stability of bacterial membranes since it can attach to their negatively loaded (anionic) phospholipids. Furthermore, it has been claimed that CHX may display an anti-inflammatory effect on neutrophil toxic products [17]. PHMB is a cationic oligomer having an average of 7–13 biguanide groups spaced by flexible hexamethylene segments (Figure 1). The high number of biguanide groups lead to a high effectiveness against microorganisms [18], although chemical characterization is difficulted for the high dispersion of oligomer sizes.

Sutures penetrate through the protective skin and can come in contact with microorganisms that grow in subcutaneous tissues such as hair follicles. Microorganisms can therefore attach to the suture surface, allowing biofilm formation and acting as a niche for subsequent infections [19-21]. Moreover, the risk of infection can be increased by an inflammatory response caused by the suture. These problems are very important for sensitive and risk applications like sutures securing a central venous catheter [21].

Currently, the most commonly used antimicrobial surgical suture is Coated Vicryl Plus Antibacterial Suture, a multifilament suture constituted by a copolymer having 90 wt-% of glycolide and 10 wt-% of L-lactide and TCS deposited on its surface to take profit of its capability to inhibit the colonization of a broad spectrum of bacteria [22]. Nevertheless, the incorporation of other bactericides is strongly recommended for the following reasons: a) The increasing resistance of bacteria to TCS caused by its massive use [23], and b) Safety issues concerning the bioaccumulation of TCS and its negative effect on immune and reproductive functions [24]. In this way, coating formulations based on an amphiphilic polymer, poly[(aminoethyl methacrylate)-*co*-(butyl methacrylate)] (PAMBM), have been proposed due to its higher antimicrobial activity at lower concentrations than that detected for TCS loaded samples [25].

CHX has been considered as alternative to TCS; specifically, coatings based on fatty acids (i.e. chlorhexidine laurate and chlorhexidine palmitate) were evaluated using Vicryl Plus as a reference multifilament suture [26]. High antimicrobial efficacy was demonstrated for up to 5 days while acceptable cytotoxic levels were determined for 11 μg/cm drug content.

The use of coatings is essential for multifilament sutures since they have a lubricant effect and can diminish tissue drag and risk of infection caused by capillarity [27,28]. These problems are not found when monofilament sutures are employed but the use of a

coating may be still highly interesting if a drug is incorporated. This is studied in the present work using Monosyn™ (i.e. polyglycolide-*b*-poly(glycolide-*co*-trimethylene carbonate-*co*-ε-caprolactone)-*b*-polyglycolide (Figure 1) abbreviated as poly(GL)-*b*-poly(GL-*co*-TMC-*co*-CL)-*b*-poly(GL)) [29] as a monofilament suture and CHX and PHMB as examples of bactericidal drugs with low and relatively high molecular weights, respectively. In addition, a new coating constituted by lactide and trimethylene carbonate (Figure 1) (abbreviated as poly(LA-*co*-TMC)) was developed according to the interest of this kind of copolymers for different biomedical applications [30-33]. Composition was selected to obtain a material with a sticky nature and a low degradation rate.

The goals of the present works involve also the evaluation of which is the best way to load the bactericide drug (i.e. direct deposition onto the suture surface or into a coating copolymer), the evaluation of the most effective biguanide compound (i.e. low or high molecular weight samples) and finally the evaluation of the higher drug load that render a bactericide /bacteriostatic effect without causing cytotoxicity.

EXPERIMENTAL SECTION

Materials

Lactide, trimethylene carbonate and $Sn(Oct)_2$ were purchased from Sigma-Aldrich. Commercially available sutures of poly(GL)-*b*-poly(GL-*co*-TMC-*co*-CL)-*b*-poly(GL) (Monosyn™, USP 0 and diameter 0.35-0.399 mm) were kindly supplied by B. Braun Surgical, S.A. This triblock copolymer was constituted by 72, 14 and 14 wt-% of glycolide, trimethylene carbonate and ε-caprolactone units, respectively. The material had a middle soft segment that represents the 43 wt-% of the sample. Weight average molecular weight was 90,700 g/mol.

All solvents, chlorhexidine (CHX), 3-(4,5-dimethylthiazol-2-yl)-2,5-diphenyl-2H-tetrazolium bromide (MTT) and cell culture labware were purchased from Sigma-Aldrich (Spain). Cosmocil® (poly(hexamethylene biguanide hydrochloride), PHMB) was kindly provided by B. Braun Surgical S.A.

The microbial culture was prepared with reagents and labware from Scharlab (Spain). *Escherichia coli* CECT 101 and *Staphylococcus epidermidis* CECT 245 bacterial strains were obtained from Spanish Collection of Type Culture (Valencia, Spain). African green monkey kidney fibroblast-like (COS-7) and epithelial-like (VERO) cells were purchased from ATCC (USA).

Polymerization

Synthesis of the coating copolymer was carried out in tubes previously silanized with a silanization solution type I (Sigma-Aldrich) to prevent chemical reaction between the monomers and the OH groups contained in the glass. Silanization was performed during 30 min and then tubes were washed three times with anhydrous methanol and dried for 24 hours in a preheated oven at 120°C. Copolymers with different ratios of lactide and trimethylene carbonate were synthesized in order to select the composition with better properties to be used as a coating.

Specifically, the selected poly(LA-*co*-TMC) copolymer having a theoretical 35 wt-% of lactide units was synthesized by bulk ring-opening polymerization of the appropriate mixture of lactide (LA) and trimethylene carbonate (TMC) for 48 h at 130 ºC under nitrogen atmosphere. $Sn(Oct)_2$ (0.1 mol /L solution in dry toluene) was used as a catalyst and the monomer/initiator (M/I) ratio was equal to 1,000. This relatively low ratio should enhance polycondensation and transesterification reactions and lead to a polymer with a random microstructure and in relatively short reaction time. When

polymerization was completed, the tube was cooled to room-temperature and the resulting copolymer was dissolved in chloroform and precipitated in methanol. The recovered material was washed several times with methanol, dried in vacuum.

Measurements

Infrared absorption spectra were recorded in the 4000-600 cm^{-1} range with a Fourier Transform FTIR 4100 Jasco spectrometer equiped with a Specac model MKII Golden Gate attenuated total reflection (ATR) cell.

^{1}H-NMR spectra were recorded with a Bruker AMX-300 spectrometer operating at 300.1 MHz. Chemical shifts were calibrated using tetramethylsilane as the internal standard and $CDCl_3$ ($\delta(^1H)$ = 7.26 ppm) and deuterated DMSO ($\delta(^1H)$ = 2.50 ppm) as solvents.

Calorimetric data were obtained by differential scanning calorimetry with a TA Instruments Q100 series with T_{zero} technology and equipped with a refrigerated cooling system (RCS). Experiments were conducted under a flow of dry nitrogen at a heating rate of 20 ºC/min with a sample weight of approximately 5 mg. Calibration was performed with indium.

Degradation studies

Prismatic pieces (1 × 1.5 × 0.02 cm^3) were employed for hydrolytic degradation while films (0.5 × 0.5 × 0.2 cm^3) were employed for enzymatic degradation in order to enhance the surface/bulk ratio. To this end, polymer samples (0.4 g) were heated at 100 ºC (i.e. clearly above its glass transition temperature) for 12 min by means of a hydraulic press equiped with heating plates and a temperature controller (Graseby Specac, Kent, England). Pressure was progressively increased from 1 to 4 bar. Samples were recovered after cooling the mold or the film to room temperature. Films were subsequently cut to the desired size.

In vitro hydrolytic degradation assays were carried in deionized water at 37 ºC, 50 ºC and 70 ºC. Samples were kept under orbital shaking in tubes filled with 8 mL of the degradation medium and sodium azide (0.03 wt-%) to prevent microbial growth for selected exposure times. The samples were then thoroughly rinsed with distilled water, dried to constant weight under vacuum and stored over P_4O_{10} before analysis. Degradation studies were performed in triplicated and the given data corresponded to the average values.

Weight retention (W_r) of the specimens was determined by the percentage ratio of weight after degradation (W_d) to initial weight before degradation (W_0):

$$W_r = W_d / W_0 \times 100 \quad (1)$$

Molecular weights were estimated by size exclusion chromatography (GPC) using a liquid chromatograph (Shimadzu, model LC-8A) equipped with an Empower computer program (Waters). A PL HFIP gel column (Polymer Lab) and a refractive index detector (Shimadzu RID-10A) were employed. The polymer was dissolved and eluted in 1,1,1,3,3,3-hexafluoroisopropanol containing CF_3COONa (0.05 M) at a flow rate of 1 mL/min (injected volume 100 µL, sample concentration 2.0 mg/mL). The number and weight average molecular weights were calculated using poly(methyl methacrylate) standards.

The enzymatic studies were carried out at 37 ºC with a *porcine* lipase (30–90 U/mg) medium and using four replicates. All samples were exposed to 1 mL of pH 7.4 phosphate buffer containing the enzyme alongside with sodium azide (0.03 *w*/*v*-%). Solutions were renewed every 48 h to prevent enzymatic activity loss. Samples were extracted, washed and dried as indicated before.

Incorporation of CHX and PHMB onto uncoated and coated poly(GL)-*b*-poly(GL-*co*-TMC-*co*-CL)-*b*-poly(GL) sutures

Poly(GL)-*b*-poly(GL-*co*-TMC-*co*-CL)-*b*-poly(GL) monofilaments (5 cm length) were immersed (during 5 s) in ethanol or methanol solutions containing different percentages of CHX (0.1-15 *w*/*v*-%) or PHMB (0.1-6 *w*/*v*-%), respectively. After drying in hot air sutures were immersed in an ethyl acetate bath containing 3 *w*/*v*-% of poly(LA-*co*-TMC) when coated samples were required. Monofilaments were finally dried and stored under vacuum.

The total amount of drug loaded was determined by dissolution of the suture and the drug in 1,1,1,3,3,3-hexafluoroisopropanol, precipitation of polymers by addition of ethanol and finally by absorbance measurements by UV spectroscopy of the resulting solution using a Shimadzu 3600 spectrometer. Calibration curves were obtained by plotting the absorbance measured at 261 and 236 nm versus CHX and PHMB concentrations, respectively.

Release experiments

Controlled release measurements were performed with 5 cm length pieces of uncoated and coated sutures. These pieces were incubated at 37 °C in an orbital shaker at 80 rpm in tubes of 10 mL for 1 week. A 3:7 *v*/*v* mixture of PBS buffer and ethanol was employed as release media, although some experiments were also carried out in an ethanol medium. Drug concentration was evaluated by UV spectroscopy as above indicated. Samples were withdrawn from the release medium at predetermined time intervals. The volume was kept constant by the addition of fresh medium. All drug release tests were carried out using three replicates and the results were averaged.

Antimicrobial test

E. coli and *S. epidermidis* bacteria were selected to evaluate the antimicrobial effect of CHX and PHMB loaded sutures. The bacteria were previously grown aerobically to exponential phase in broth culture (5 g/L beef extract, 5 g/L NaCl, 10 g/L tryptone, pH 7.2).

Growth experiments were performed on a 24-well culture plate. 5 pieces of 1 cm length of uncoated and coated sutures were placed into each well. Then, 2 mL of broth culture containing 10^3 CFU was seeded on the suture samples. The cultures were incubated at 37 °C and agitated at 160 rpm. Aliquots of 100 µl were taken at predetermined time intervals for absorbance measurement at 650 nm in a plate reader. Thus, turbidity was directly related to bacterial growth.

Bacterial adhesion onto sutures was also determined. The culture media were aspirated after incubation and the material washed once with distilled water. Then, 0.5 mL of sterile 0.01 M sodium thiosulfate was added to each well and afterwhich the sutures were removed. After the addition of 1 mL of broth culture, the plate was incubated at 37 °C and agitated at 160 rpm for 24 h. The bacterial number was determined as above indicated. All assays were conducted in quadriplicate and the values averaged.

Regarding the qualitatively method, around 5 cm length pieces of loaded and unloaded sutures were placed into the agar diffusion plate and, seeded with 10^4 CFU/mL of both bacteria separately. The culture medium was prepared with 10.6 g of Brilliant Green Agar (BGA. Scharlau) or 7.9 g of Violet Red Bill Dextrose Agar (VRBDA, Scharlau) dissolved in 200 mL of Milli-Q water and sterilized at 121 ºC for 30 min in an autoclave. Plates were filled with 15 mL of medium and kept at rest to solidify the medium at room temperature. Inhibition halos images were taken after incubation of samples with bacteria for 24 h at 37 ºC.

Cell adhesion and proliferation assays

Studies were performed with fibroblast-like COS-7 cells and epithelial Vero cells. In all cases, cells were cultured in Dulbecco's modified Eagle medium (DMEM) as previously reported.[34]

5 pieces of 1 cm length of uncoated and coated sutures were placed and fixed in each well of a 24-well culture plate with a small drop of silicone (Silbione® MED ADH 4300 RTV, Bluestar Silicones France SAS, Lyon, France). This plate was then sterilized by UV-radiation in a laminar flux cabinet for 15 min. For the cell adhesion and proliferation assays, aliquots of 50–100 μL containing 2×10^5 cells were seeded onto the samples in each well and incubated for 24 h (adhesion assay) or 96 h (proliferation assay).

Samples were evaluated by the standard adhesion and proliferation method [34]. The used procedure is based on a simple modification of the ISO10993-5:2009 standard test that describes the appropriate methodology to assess the *in vitro* cytotoxicity of medical devices. This test is designed to determine the *in vitro* biological response of mammalian cells using appropriate biological parameters. According to this ISO standard, devices are placed in one of three categories based on the expected contact with the patient: a) Limited (≤24 h), b) Prolonged (>24 h and ≤30 days) and c) Permanent (>30 days). In our case, the assay was performed according to both limited and prolonged categories. The study was carried out using four replicates and the results were averaged. Samples with adhered and grown cells on the samples were fixed with 2.5 *w*/*v*-% formaldehyde at 4 °C overnight. They were subsequently dehydrated and processed for observation of cell morphology.

Scanning electron microscopy (SEM) was employed to examine the morphology of coated and uncoated sutures as well as the morphology of adhered cells onto them. Carbon

coating was accomplished with a Mitec k950 Sputter Coater (fitted with a film thickness monitor k150x (Quorum Technologies Ltd., West Sussex, UK). SEM micrographs were obtained with a Zeiss Neon 40 EsB instrument (Carl Zeiss, Oberkochen, Germany).

Statistical analysis

Values were averaged and graphically represented, together with their respective standard deviations. Statistical analysis was performed by one-way ANOVA test to compare the means of all groups, and then Tukey's test was applied to determine a statistically significant difference between two groups. For it, the Origin software (OriginPro v.8, OriginLab Corporation, Northampton, MA, USA) was used with a test confidence level at 95% ($p < 0.05$).

RESULTS AND DISCUSSION

Synthesis and characterization of the coating poly(LA-*co*-TMC) copolymer

The copolymer that exhibited better coating properties was that having a lactide content of 30-35 wt-%. Other compositions rendered coatings that were too rigid and easily detached from the suture surface (e.g. 50 wt-% of lactide) or too sticky for proper handling of the suture (e.g. 20 wt-% of lactide).

A reaction temperature of 130 ºC was enough to guarantee complete conversion of monomers in a reasonable time and avoid thermal degradation. The progress of the reaction could be easily followed from ^{1}H NMR spectra taken from aliquots of the reaction mixture at regular time intervals. Thus, spectra recorded at the beginning of copolymerization showed signals of unreacted lactide (5.43 and 1.22 ppm) and trimethylene carbonate (4.43 and 1.98 ppm) monomers, which can be easily distinguished from those corresponding to units incorporated into the polymer chain (5.25–4.95 and 1.61–1.52 ppm for methine and methyl protons of lactic acid units (L); 4.20–4.10 ppm for

the α- and γ-methylene protons and 2.10–1.90 ppm for the β-methylene protons of trimethylene carbonate units (TMC)) (Figure 2). Lactide reacted faster, and consequently polymerization time was determined by the achievement of a complete conversion of trimethylene carbonate, as shown in the spectrum of Figure 2 [35].

The areas of peaks at 5.20–4.90 ppm and 4.20–4.10 ppm were used to determine the final composition of lactide units:

$$LA\ (wt\text{-}\%) = A_{5.20–4.90} \times 72 / [(A_{5.20–4.90} \times 72) + (A_{4.20–4.10} \times 102 /4)] , \qquad (2)$$

where 72 and 102 are the molecular weights of lactyl and trimethyl carbonyl units, respectively.

Values were slightly lower than the theoretical monomer feed ratio due to a practically negligible sublimation of lactide. Thus, 32-34 wt-% was determined when the feed ratio corresponded to 35 wt-%.

Sequence sensitivity was found for methine and methyl protons, and consequently information of chain microstructure could be derived, as previously reported [36].

The proton spectrum showed an intense multiplet at around 5.18 ppm, which was attributed to L**L**L and Tmc**L**L triads, together with a quintuplet around 5.03 ppm caused by the overlapping of quadruplets associated with L**L**Tmc and Tmc**L**Tmc triads. In addition, doublets corresponding to the L**L** and Tmc**L** sequences could be detected at around 1.60 and 1.53 ppm, respectively, in agreement with the reported dyad sensitivity of CH_3 protons. Note that the upfield dyad has a clearly higher intensity, indicating a high ratio of Tmc**L**Tmc sequences in the copolymer. This triad results from transesterification reactions inside the lactidyl units and should be favored by temperature, time and catalysts.

The copolymer was obtained with a weight average molecular weight of 145,000 g/mol and a polydispersity index of 2.3. The FTIR spectrum was in full agreement with the expected chemical constitution, displaying the characteristic common bands of both

homopolymers (e.g. carbonyl group at 1735-1745 cm^{-1}) as well as those only associated with polylactide or polytrimethylene carbonate (Figure 3) [37,38]. The main peculiar difference, which may be a consequence of molecular interactions, is the decrease of the 1080 cm^{-1} band (i.e. symmetric C-O-C stretching) that usually appears with higher intensity in the PLA homopolymer.

The DSC calorimetric trace (Figure 4) revealed the amorphous character of the copolymer since only a glass transition temperature of -20 ºC could be detected. This temperature was close to that reported for poly(trimethylene carbonate) (i.e. -25ºC [39] and -32 ºC [40]) and far from the value of 60 ºC for polylactide, as could be expected from the chemical composition. Thermal behavior was clearly different from that of the polymer matrix, which showed a glass transition temperature of -14 ºC and great ability to crystallize from the glassy state, giving rise to polyglycolide crystalline entities with a melting point close to 198 ºC (Figure 4).

The copolymer was hydrolytically and enzymatically degradable, as could be inferred from both the sample weight (Figure 5) and molecular weight losses (Figure 6) observed during exposure to the different degradation media. Thus, three phases were observed for the pH 7 medium under the accelerated condition provided by a temperature of 70 ºC. Initially, the sample weight decreased very slowly, and approximately 24 days were required to produce a loss of 9%. After this period, a very fast weight loss was observed as degradation after the previous step was sufficiently advanced to render a high proportion of soluble molecular fragments. Specifically, weight loss increased from 9% to 83% between days 24 and 34. The third step was again slow because it involved highly insoluble and crystalline low molecular weight residues. Only the first step was detected up to 83 days, when degradation was performed at 50 ºC; in particular, a loss of 18% was determined. Practically no weight loss was detected at the physiological temperature of 37 ºC at the

maximum exposure time (i.e. 83 days). A low susceptibility to enzymatic degradation was also found since a weight loss of only 7% was determined after 61 days of exposure.

Molecular weight changes were very useful to verify the progress of degradation. Thus, a steady decrease was observed in a first degradation step for hydrolytic degradation at the three test temperatures. This step followed a first-order kinetic which could be associated with a random chain scission mechanism. Obviously, the kinetic constant increased with temperature. In a second step, the molecular weight reached a practically constant value that can be interpreted as the minimum molecular size of insoluble degraded fragments. Thus, a molecular weight of 3,000 g/mol was attained after 24 days of exposure to the medium at 70 ºC, whereas 65 days were required to achieve a constant molecular weight of 7,100 g/mol at a temperature of 50 ºC. Note that this molecular weight was slightly higher than that observed at 70 ºC due to the different solvent capability.

The evolution of the polydispersity index (inset of Figure 6) was also useful to follow the degradation process since it reached a maximum value at the end of the first degradation step. After this period, samples became more homogeneous due to solubilization of small fragments and degradation of high molecular weight chains.

Results pointed out a great difference between enzymatic and hydrolytic degradation under physiological conditions. It is obvious that hydrolytical degradation was not significant under these conditions and consequently small changes derived from using a distilled water medium which progressively becomes acid during degradation or a buffered pH 7.4 medium could be considered negligible.

CHX and PHMB loading of poly(GL)-*b*-poly(GL-*co*-TMC-*co*-CL)-*b*-poly(GL) monofilament sutures

The selected drugs (CHX and PHMB) had a hydrophilic character that contrasted with the hydrophobicity of the selected coating copolymer. Therefore, a relatively volatile and economical common solvent could not be used for the copolymer and the drugs. Ethyl acetate, ethanol and methanol were selected for coating and loading baths containing poly(LA-*co*-TMC), CHX and PHMB, respectively. Thus, the drug loading process involved two steps: incorporation of CHX or PHMB and coating, if necessary. Immersion time (5 s), drying method (hot air stream) and copolymer concentration (3 *w*/*v*-%) were optimized to obtain the most economical and fastest process, as well as completely coated and uniform sutures. For example, Figure 7a shows that a higher copolymer concentration (e.g. 10 *w*/*v*-%) leads to formation of some aggregates on the monofilament surface. Drug particles can be detected on the suture surface after the first immersion, with these non-homogeneities being clearer for PHMB (Figure 7b). Nevertheless, uniform surfaces were achieved after incorporation of the coating, as shown in Figure 7c.

Good correlation was observed between the drug concentration in the alcohol bath and the amount of loaded drug referred to the suture unit length (Figure 8). The slope of linear plots was 1.12 and 1.13 for CHX and PHMB, respectively, where 0.98-0.99 was the value of the determination coefficient (r^2). These similar slopes indicated that the amount of incorporated drug was independent of its nature, as could be expected from the high chemical similarity of both biguanide compounds and the fact that the loaded amount should be mainly determined by the suture surface (i.e. diameter of the suture or USP number) [33].

For the sake of completeness, Figure 8 also shows the correlation for uncoated samples (i.e. when the drug was merely adsorbed on the fiber surface after the first bath). In this case, the determination coefficient decreased, and specifically a value of 0.92 was

found for PHMB. It seems that the relatively high deviation from a perfect linear plot is due to an easy desorption during the manipulation of a suture lacking the protective coating. Note also that in the case of CHX the slope decreased to 1.00, suggesting again some loss of the absorbed drug during manipulation. It is, however, important to emphasize the protective effect of the selected coating, together with the fact that drugs loaded in the first bath remained adsorbed on the suture during the coating step due to their complete insolubility in the ethyl acetate bath. It should also be pointed out that the amount of loaded drug was even greater (CHX in Figure 8a) when the coating was employed even though the process required an additional bath.

CHX and PHMB release from poly(GL)-*b*-poly(GL-*co*-TMC-*co*-CL)-*b*-poly(GL) monofilament sutures

The release of PHMB and CHX was studied using a medium consisting of a 3:7 *v*/*v* mixture of PBS buffer and ethanol since it was a better solvent for the selected drugs than a typical nutrient serum medium. In this sense, there are previous studies that have reported this type of release, being Zurita et al. [33] who first pointed out this fact. It was also determined that physiological medium supplemented with ethanol accelerated the release of hydrophobic drugs and allowed performing kinetic studies in short-term experiments. Figure 9a compares PHMB release percentages for uncoated and coated sutures at given drug load (i.e. ~ 6.8 μg/cm). Results clearly demonstrated the effectiveness of the coating to suppress the burst effect. In fact, 83% of the drug was released from the uncoated suture in only 5 min, while a decrease to 5% was determined when poly(LA-*co*-TMC) was used as a coating. In this case, total release was achieved after 1 h of exposure. The release was enhanced when 100% ethanol was used, with complete release being achieved after 45

min. Nevertheless, even in this case the coating was appropriate to suppress the burst effect.

The release of CHX was faster, as shown by comparing the samples loaded with a similar amount of PHMB and CHX in Figure 9a. It can also be seen that CHX was not completely released. Thus, a small amount of the drug was effectively adsorbed in the suture (i.e. 16% (Figure 9b) for the sample loaded with ~ 5.6 μg/cm, which means a value close to 0.9 μg/cm).

Figure 9b illustrates the change in the release profiles for samples loaded with different amounts of CHX. All profiles showed a fast release step with a slope that slightly increased with concentration and a different percentage of retained drug (i.e. a plateau level was detected). This percentage always corresponded to an adsorption around 0.9 μg/cm. Thus, it was an intrinsic characteristic of physicochemical interactions that could be established between CHX and the polymer matrix. Note that the plateau observed in the release curves could not be associated with a solubility problem since samples loaded with a higher amount of CHX should have lower release percentages.

For the sake of completeness, Figure 9b also plots the release profile of an uncoated suture. This sample incorporated approximately 5 μg/cm of CHX, according to the loading relationship of Figure 8, and consequently the observed release percentage of 82% indicated that again 0.9 μg/cm of CHX remained adsorbed on the suture surface. Therefore, the coating is not relevant for retaining the amount of CHX corresponding to the plateau, which should be mainly due to interactions with poly(GL)-*b*-poly(GL-*co*-TMC-*co*-CL)-*b*-poly(GL).

Antimicrobial effect of CHX and PHMB loaded poly(GL)-*b*-poly(GL-*co*-TMC-*co*-CL)-*b*-poly(GL) monofilament sutures

The antimicrobial effect of CHX and PHMB loaded sutures was quantitatively evaluated following the growth kinetics of Gram-negative (*E.coli*) and Gram-positive (*S. epidermidis*) bacteria. Figure 10 shows that, for both types of bacteria, bacterial growth on the coated suture was always similar to that of the control. This growth was characterized by a lag or latency phase for a period of 4 h followed by a typical exponential growth (log phase). Therefore, the results showed that the coated suture was highly susceptible to bacterial infection. For this reason, it seemed interesting to incorporate CHX or PHMB to suppress this effect. Sutures loaded in baths with a drug concentration of 0.1 *w*/*v*-% (equivalent to a load of 0.112 μg/cm and 0.113 μg/cm for CHX and PHMB, respectively) did not have any growth inhibitory effect. In fact, concentrations of 0.3 *w*/*v*-% and 1 *w*/*v*-% were required for PHMB and CHX, respectively, to lead to a bacteriostatic effect. This effect was characterized by an increased duration of the lag phase up to 10 h and a subsequent linear growth instead of the typical exponential growth. The observed linear relationship basically indicates that bacterial growth increases as the drug is consumed. The bactericide effect was found for PHMB and CHX concentrations in the baths of 1.5 *w*/*v*-% and 5 *w*/*v*-% or higher, respectively. In these cases, the latency phase was around 30 h and the maximum growth after 48 h of culture was 20%. A completely inhibitory effect required a minimum CHX and PHMB concentration of 10 *w*/*v*-% and 3 *w*/*v*-%, respectively, which means a load of 11.2 μg/cm and 3.4 μg/cm.

The behavior of uncoated CHX and PHMB loaded sutures was similar for some representative samples (i.e. sutures loaded with the amount corresponding to a bacteriostatic effect), as shown in Figure 10. In fact, a lower inhibition with respect to coated sutures can be explained considering that the amount of drug loaded in the bath was lower than expected (Figure 8), especially in the case of CHX.

Evaluation of bacterial adhesion was carried out as another antimicrobial control for the new materials (Figure 11). Results demonstrated a dose-dependent effect for both Gram-negative and Gram-positive bacteria. Therefore, adhesion was not inhibited for sutures coming from baths containing 0.1 *w*/*v*-% of drugs, while partial adhesion in the 40%-60% range was found for sutures coming from baths containing 5 *w*/*v*-% and 0.3-1.5 *w*/*v*-% of CHX and PHMB, respectively. Finally, complete inhibition was observed for the high doses corresponding to baths containing 10-15 *w*/*v*-% and 3-6 *w*/*v*-% of CHX and PHMB. Inhibition was higher for coated than uncoated sutures because of higher drug loading efficiency (Figure 8).

The above results could also be qualitatively observed in the Agar tests by measurement of the inhibition halos around sutures (Figure 12). These halos are a consequence of the bactericidal activity which affects both inhibition of bacterial growth and bacterial adhesion on the suture. It should be considered that this test subestimates the effect produced by cationic antimicrobial compounds since they have a limited diffusion in the lipophilic agar medium. Nevertheless, results clearly showed that CHX and PHMB have a preferential effect against Gram-positive bacteria, which exhibited clearly greater inhibition halos than the Gram-negative medium.

Differences in activity against Gram-positive bacteria between CHX and PHMB were reflected by the greater inhibition halos of CHX, probably caused by easy diffusion of lower molecular sizes through the agar medium. Note that an opposite behavior can be deduced from growth kinetic measurements, a feature that can be explained by a high diffusion rate for the lower molecular weight drug. Finally, the behavior of coated and uncoated sutures was always similar. This demonstrates that the selected coating did not hinder drug diffusion from the suture to the medium, which was independent of drug size (small and big for CHX and PHMB, respectively).

Cytotoxicity of CHX and PHMB loaded poly(GL)-*b*-poly(GL-*co*-TMC-*co*-CL)-*b*-poly(GL) monofilament sutures

Cytotoxicity was evaluated using cell lines with a high proliferative capacity. Specifically, COS-7 and Vero cells were selected in this study because they have well-differentiated morphologies, namely elongated (fibroblast-like) and polygonal (epithelial-like) shapes, respectively. These cells show different forms of adhesion to a material surface and provide complementary information. Fibroblasts can adhere by focal joints, while epithelial adhere using a wide extension of cell membrane. Cell adhesion and cell proliferation events after 24 and 96 h of culture, respectively, were analysed to determine the cytotoxicity of drug loaded sutures (Figure 13).

Adhesion of both cell lines was reduced in the 40% - 60% range when sutures were loaded with the amount of CHX that rendered a bactericidal effect and even for the lowest load leading to a bacteriostatic effect. Cell proliferation assays were more useful to discriminate between the different loads. Thus, samples coming from baths having 5 *w*/*v*-% or higher percentages of CHX reduced cell viability drastically, whereas those loaded from a bath with a 1 *w*/*v*-% allowed a cell growth similar to that observed for the control and the unloaded suture (Figures 13e and 13f).

On the other hand, the incorporation of PHMB reduced cell adhesion in the 20% - 40% range for both types of cell lines, which was practically independent of the amount of loaded drug (Figures 13c and 13d). Furthermore, bactericidal and bacteriostatic doses of PHMB caused a decrease close to 60% in the cell proliferation assays (Figures 13g and 13h). Differences with CHX results demonstrated that a low molecular size of biguanide compounds had adverse effects on cell growth, as can be expected from differences in the ability to penetrate into the cells. The results indicated that the use of coated sutures favored cell adhesion and proliferation, as can be clearly seen in Figures 13d and 13g.

Micrographs in Figure 14 show the morphology of epithelial-like and fibroblast-like cells adhered to drug loaded sutures. In general, epithelial like cells appear widely extended, forming clusters while fibroblast-like cells appear as single, extended, well distributed cells.

CONCLUSIONS

A random copolymer prepared by ring opening polymerization of 35 wt-% of lactide and 65 wt-% of trimethylene carbonate showed appropriate characteristics to be used as a coating of monofilament sutures such as the poly(GL)-*b*-poly(GL-*co*-TMC-*co*-CL)-*b*-poly(GL) three block copolymer. The new coating was characterized by a T_g close to -20 ºC, a low degradation rate at room temperature in a pH 7.4 medium and a solubility in organic media enabling a consistent and homogeneous coating to be obtained by immersion of sutures in an ethyl acetate bath.

Antimicrobial drugs such as CHX and PHMB can be directly adsorbed on the suture surface or loaded into the suture by a two-step procedure involving a subsequent coating. The second method showed advantages in terms of loading efficiency as drugs were more protected against detachment caused by handling. Furthermore, the coating was essential to avoid a complete burst effect in the case of PHMB. CHX was released according to a first relatively fast step and at a rate slightly dependent on the amount of loaded drug. However, in all cases an amount close to 0.9 μg/cm was retained on the suture surface, probably as a consequence of good interactions with the polymer matrix. The selected drugs exhibited a dose-dependent antimicrobial activity, and it was possible to distinguish between bacteriostatic and bactericidal activity. Bacterial growth kinetics and bacterial adhesion measurements indicated greater activity of PHMB against Gram-positive bacteria when samples with similar loaded weights of CHX and PHMB were compared.

Incorporation of the coating was not essential in terms of bactericidal activity if the effect of lower drug loading efficiency was discarded.

Cell adhesion and cell proliferation assays demonstrated the potential cytotoxicity of sutures having high doses of CHX and PHMB, while those with a clear bacteriostatic effect (i.e. inhibition of bacterial growth for a period between 10 h – 30 h) could fortunately be considered non-cytotoxic. The presence of the coating copolymer was more beneficial to reduce cytotoxicity, especially when the higher molecular weight PHMB was employed since the molecular size influenced the rate of diffusion towards cells.

In summary, sutures loaded with biguanide derivatives such as CHX and PHMB exhibited a clear preventive effect against bacterial infection or colonization while allowing cell adhesion and proliferation in regenerated tissues.

Acknowledgements. Authors are in debt to supports from MINECO and FEDER (MAT2015-69547-R) and the Generalitat de Catalunya (2014SGR188). The work has also been carried out under a research agreement between B. Braun Surgical, S. A. and the Universitat Politècnica de Catalunya. Ms Y. Márquez thanks financial support from B. Braun Surgical S.A.

REFERENCES

1. D. Davies, Understanding Biofilm Resistance to Antibacterial Agents. Natur. Rev. Drug Discov. 2 (2003) 114-122.

2. G. Sun G, Prevention of Hospital and Community Acquired Infections by Using Antibacterial Textiles and Clothing. In: Polymeric Materials with Antimicrobial Activity, A. Muñoz-Bonilla, M.L. Cerrada, M. Fernández-García, Eds., RSC Polym. Chem. S. Ch 6 (2014) 139-154.

3. J.W. Costerton, P.S. Stewart, E.P. Greenberg, Bacterial Biofilms: A Common Cause of Persistent Infections. Science 284 (1999) 1318-1322.

4. L. Chen, L. Bromberg, T. A. Hatton, G. C. Rutledge, Electrospun Cellulose Acetate Fibers Containing Chlorhexidine as a Bactericide. Polymer 49 (2008) 1266-1275.

5. L. J. del Valle, L. Franco, R. Katsarava, J. Puiggalí, Electrospun Biodegradable Polymers Loaded with Bactericide Agents. AIMS Materials Science (2016) *in press*.

6. A. M. Lenz, M. Fairweather, W. G. Cheadle, Resistance Profiles in Surgical-Site Infection. Future Microbiol. 3 (2008) 453– 462.

7. F. R. DeLeo, H. F. Chambers, Reemergence of Antibiotic-Resistant *Staphylococcus aureus* in the Genomics Era. J. Clin. Invest. 119 (2009) 2464-2474.

8. E. C. J. Broex, A. D. I. van Asselt, C. A. Bruggeman, F. H. van Tiel, Surgical Site Infections: How High Are The Costs? J. Hosp. Infect. 72 (2009) 193– 201.

9. P. N. Danese, Antibiofilm Approaches: Prevention of Catheter Colonization. Chem. Biol. 9 (2002) 873–880.

10. S. Abedon, S. Kuhl, B. Blasdel, E. Martin Kutter, Phage Treatment of Human Infections. Bacteriophage 1 (2011) 66–85.

11. A. Melaiye, Z. Sun, K. Hindi, A. Milsted, D. Ely, D. H. Reneker, C. A. Tessier, W. J. Youngs, Silver(I)−Imidazole Cyclophane gem-Diol Complexes Encapsulated by Electrospun Tecophilic Nanofibers: Formation of Nanosilver Particles and Antimicrobial Activity. J Am Chem Soc 127 (2005) 2285-2291.

12. G. J. Baley, G. E. Peck, G. S. Banker, Bactericidal Properties of Quaternary Ammonium Compounds in Dispersed Systems. J. Pharm. Sci. 66 (1977) 696-699.

13. L. F. Ortenzio, L. S. Stuart, The Behavior of Chlorine-Bearing Organic Compounds in the AOAC Available Chlorine Gemicidal Equivalent Concentration Test. J. Assoc. Off. Ana. Chem. 42 (1959) 630-633.

14. I. Chopra, M. Roberts, Tetracycline Antibiotics: Mode of Action, Applications, Molecular Biology, and Epidemiology of Bacterial Resistance. Microbiol. Mol. Biol. Rev. 65 (2001) 232–260.

15. J. B. Leikin, F. P. Paloucek, "Chlorhexidine Gluconate", Poisoning and Toxicology Handbook (4th ed.), Informa (2008) 183–184.

16. J.B.D. Green, T. Fulghum, M.A. Nordhaus, Immobilized Antimicrobial Agents: A Critical Perspective, In: Science Against Microbial Pathogens: Communicating Current Research and Technological Advances, Formatex Microbiology Books Series, Méndez-Vila E, Ed. (2011) Badajoz (Spain).

17. F. Montecucco, M. Bertolotto, L. Ottonello, A. Pende, P. Dapino, A. Quercioli, F. Mach, F. Dallegri, Chlorhexidine Prevents Hypochlorous Acid-Induced Inactivation of Alpha1-Antitrypsin. Clin Exp Pharmacol Physiol. 36 (2009) 72-77.

18. K. Kaehn, Polihexanide: A Safe and Highly Effective Biocide. Skin Pharmacol. Physiol. 23 (2010) 7–16.

19. S. Katz, M. Izhar, D. Mirelman, Bacterial Adherence to Surgical Sutures. A Possible Factor in Suture Induced Infection. Ann. Surg. 194 (1981) 35–41.

20. R.M. Donlan, J.W. Costerton, Biofilms: Survival Mechanisms of Clinically Relevant Microorganisms. Clin. Microbiol. Rev. 15 (2002) 167–193.

21. J. Tarja, Karpanen, A. L. Casey, T. Whitehouse, P. Nightingale, I. Das, T.S.J. Elliott, Clinical Evaluation of a Chlorhexidine Intravascular Catheter Gel Dressing on Short-Term Central Venous Catheters. Am. J. Infect. Control 44 (2016) 54–60.

22. M. L. Storch, S. J. Rothenburger, G. Jacinto, Experimental Efficacy Study of Coated VICRYL Plus Antibacterial Suture in Guinea Pigs Challenged with *Staphylococcus aureus*. Surg. Infect. 5 (2004) 281–288.

23. S. P. Yazdankhah, A. A. Scheie, E. A. Hoiby, B. T. Lunestad, E. Heir, T. O. Fotland, K. Naterstad, H. Kruse, Triclosan and Antimicrobial Resistance in Bacteria: An Overview. Microb. Drug Resist. 12 (2006) 83−90.

24. A. E. Aiello, E. M. R. Clayton, M. Todd, J. B. Dowd, The Impact of Bisphenol A and Triclosan on Immune Parameters in the U.S. Population, NHANES 2003−2006. Environ. Health Perspect. 119 (2011) 390−396.

25. Y. Li, K.N. Kumar, J.M. Dabkowski, M. Corrigan, R.W. Scott, K. Nüsslein, G.N. Tew, New Bactericidal Surgical Suture Coating. Langmuir 28 (2012) 12134-12139.

26. A. Obermeier, J. Schneider, S. Wehner, F. D. Matl, M. Schieker, R. Von Eisenhart-Rothe, A. Stemberger, R. Burgkart, Novel High Efficient Coatings for Anti-Microbial Surgical Sutures Using Chlorhexidine in Fatty Acid Slow-Release Carrier Systems. PLOS one 9 (2014) e101426.

27. C. A. Homsy, K. E. McDonald, W. W. Akers, Surgical Suture-Canine Tissue Interaction for Six Common Suture Types. J. Biomed. Mater. Res. 2 (1968) 215-230.

28. H. P. Hirshman, D. Schurman, G. Kajiyama, Penetration of *Staphylococcus aureus* into Sutured Wounds. J. Orthopaed. Res. 2 (1984) 269-271.

29. S. Oberhoffner, H. Planck, Surgical Suture Material from Triblockterpolymer, its Use in Surgery and Process for its Preparation. (1996) EP 0835895B1.

30. A. Södergård, M. Stolt, Properties of Lactic Acid Based Polymers and their Correlation with Composition. Prog. Polym. Sci. 27 (2002) 1123-1163.

31. D. W. Grijpma, Q. Hou, J. Feijen, Preparation of Biodegradable Networks by Photo-Crosslinking Lactide, ε-Caprolactone and Trimethylene Carbonate-Based Oligomers Functionalized with Fumaric Acid Monoethyl Ester. Biomaterials 26 (2005) 2795-2802.

32. J. Cai, K. J. Zhu, S. L. Yang, Surface Biodegradable Copolymers – Poly(D,L-lactide-*co*-1-methyl-1,3-trimethylene carbonate) and Poly(D,L-lactide-*co*-2,2-dimethylene carbonate): Preparation, Characterization and Biodegradation Characteristics *in vivo*. Polymer 39 (1998) 4409-4415.

33. R. Zurita, A. Rodríguez-Galán, J. Puiggalí, Triclosan Release from Coated Polyglycolide Threads. Macromol. Biosci. 6 (2005) 58-69.

34. E. Llorens, L.J. del Valle, A. Díaz, M.T. Casas, J. Puiggalí, Polylactide Nanofibers Loaded with Vitamin B6 and Polyphenols as Bioactive Platform for Tissue Engineering. Macromol. Res. 21 (2013) 775–787.

35. L. Franco, S. Bedorin, J. Puiggalí, Comparative Thermal Degradation Studies on Glycolide/Trimethylene Carbonate and Lactide/Trimethylene Carbonate Copolymers. J. Appl. Polym. Sci. 104 (2007) 3539–3553.

36. D. R. Draney, P. K. Jarrett, Polym. Prepr. (Am. Chem. Soc., Div. Polym Chem.) 31 (1990) 137-138.

37. G. Kister, G. Cassanas, M. Vert, Effects of Morphology, Conformation and Configuration on the IR and Raman Spectra of Various Poly(lactic acid)s. Polymer 39 (1998) 267-273.

38. H. Wang, J. H. Dong, K. Y. Qiu, Synthesis and Characterization of ABA-Type Block Copolymer of Poly(trimethylene carbonate) with Poly(ethylene glycol): Bioerodible Copolymer. J. Polym. Sci. Part A: Polym. Chem. 36 (1998) 695–702.

39. J.H. Kim, J.H. Lee, Preparation and Chain-Extension of P(LLA-*b*-TMC-*b*-LLA) Triblock Copolymers and their Elastomeric Properties. Macromol. Res. 10 (2002) 54-59.

40. C. Sanson, J.F. Le Meins, C. Schatz, A. Soum, S. Lecommandoux, Temperature Responsive Poly(trimethylene carbonate)-*block*-poly(L-glutamic acid) Copolymer: Polymersomes Fusion and Fission. Soft Matter. 6 (2010) 1722-1730.

FIGURE CAPTIONS

Figure 1. Chemical structures of poly(GL)-*b*-poly(GL-*co*-TMC-*co*-CL)-*b*-poly(GL) (Monosyn^{TM}), the coating poly(LA-co-TMC) copolymer and the selected CHX and PHMB bactericides.

Figure 2. ^{1}H NMR spectrum of the coating copolymer with indication of peaks associated with trimethylene carbonate (T) and acid lactic (L) units as labeled in the chemical formula. Small arrow points to the presence of a minor amount of trimethylene carbonate monomer for samples taken at a reaction time slightly shorter than that corresponding to a complete conversion.

Figure 3. FTIR spectra (2050-650 cm^{-1}) of PLA, PTMC and the synthesized copolymer. Characteristic peaks of PLA and PTMC are indicated by red and green dashed lines, respectively, whereas common peaks are indicated by the blue dashed lines.

Figure 4. DSC heating traces of poly(GL)-*b*-poly(GL-*co*-TMC-*co*-CL)-*b*-poly(GL) (down) and the coating copolymer (up).

Figure 5. Remaining weight percentage of poly(LA-*co*-TMC) coating sample exposed to a pH 7.4 hydrolytic degradation medium at 70 ºC (▲), 50 ºC (■) and 37 ºC (●) and a porcine pancreatic lipase enzymatic medium (◊).

Figure 6. Changes in the weight average molecular weight of poly(LA-*co*-TMC) coating sample exposed to a pH 7.4 hydrolytic degradation medium at 70 ºC (▲), 50 ºC (■) and 37 ºC (●). Changes in the polydispersity index during accelerated degradation are shown in the inset.

Figure 7. Scanning electron micrographs of a monofilament of the poly(GL)-*b*-poly(GL-*co*-TMC-*co*-CL)-*b*-poly(GL) suture with the following treatments: a) coating by

immersion for 5 s in an ethyl acetate bath containing 10 *w*/*v*-% of poly(LA-*co*-TMC), b) immersion in a methanol bath containing 3 *w*/*v*-% of PHMB and c) a first immersion in a methanol bath containing 3 *w*/*v*-% of PHMB and then in an ethyl acetate bath containing 3 *w*/*v*-% of poly(LA-*co*-TMC) (c).

Figure 8. Plot of the amount of chlorhexidine (●) and PHMB (■) incorporated into the poly(GL)-*b*-poly(GL-*co*-TMC-*co*-CL)-*b*-poly(GL) suture (drug weight/suture length) versus drug concentration of ethanol and methanol baths. Results are given for solutions with (solid lines) and without (dashed lines) poly(LA-*co*-TMC).

Figure 9. a) PHMB release percentages in PBS-EtOH 30:70 medium for uncoated (○) and coated (●) sutures. For the sake of completeness, data for an EtOH medium are also plotted (▲) for the coated suture as well as the CHX release percentage plot in PBS-EtOH 30:70 medium for the coated suture (■). Samples were obtained from baths containing 6 *w*/*v*-% and 5 *w*/*v*-% of PHMB and CHX, respectively. b) CHX release percentages in a PBS-EtOH 30:70 medium for coated sutures loaded in baths with 15 *w*/*v*-% (♦),10 *w*/*v*-% (●), 5 *w*/*v*-% (■) and 1 *w*/*v*-% (▲) of CHX. For the sake of completeness, data for an uncoated suture coming from a bath containing 5 *w*/*v*-% (□) of CHX are also plotted.

Figure 10. Growth curves of *E. coli* (a,c) and *S. epidermidis* (b,d) on culture plate as positive control (□), coated suture as blank (○) and poly(LA-*co*-TMC) coated sutures (dashed lines) loaded in baths with the indicated *w*/*v*-% of CHX (a,b) and PHMB (c,d). For the sake of completeness, data for uncoated sutures loaded from selected baths are also plotted (solid lines).

Figure 11. Adhesion of *E. coli* (a,c), and *S. epidermidis* (b,d) bacteria on uncoated (gray bars) and poly(LA-*co*-TMC) coated (grid bars) sutures loaded in baths with the indicated

concentrations of CHX (a,b) and PHMB (c,d). Data concerning the culture plate as positive control and the coated and uncoated sutures as blank are also provided.

Figure 12. Agar tests showing the inhibition zone of *E. coli* and *S. epidermidis* bacteria caused by uncoated and poly(LA-*co*-TMC) coated sutures loaded in baths with the indicated CHX and PHMB concentrations.

Figure 13. Adhesion (a-d) and proliferation (e-h) of Vero (a,c,e,g) and COS-7 (b,d,f,h) cells on uncoated (gray bars) and poly(LA-*co*-TMC) (grid bars) coated sutures loaded in baths with the indicated concentrations of CHX (a,b,e,f) and PHMB (c,d,g,h). Data concerning the culture plate as positive control are also provided.

Figure 14. SEM micrographs of Vero (a,b) and COS-7 (c) cell growth on poly(LA-*co*-TMC) coated sutures loaded in baths with CHX (a,b) and PHMB (c) concentrations of 1 *w*/*v*-% and 1.5 *w*/*v*-%, respectively.

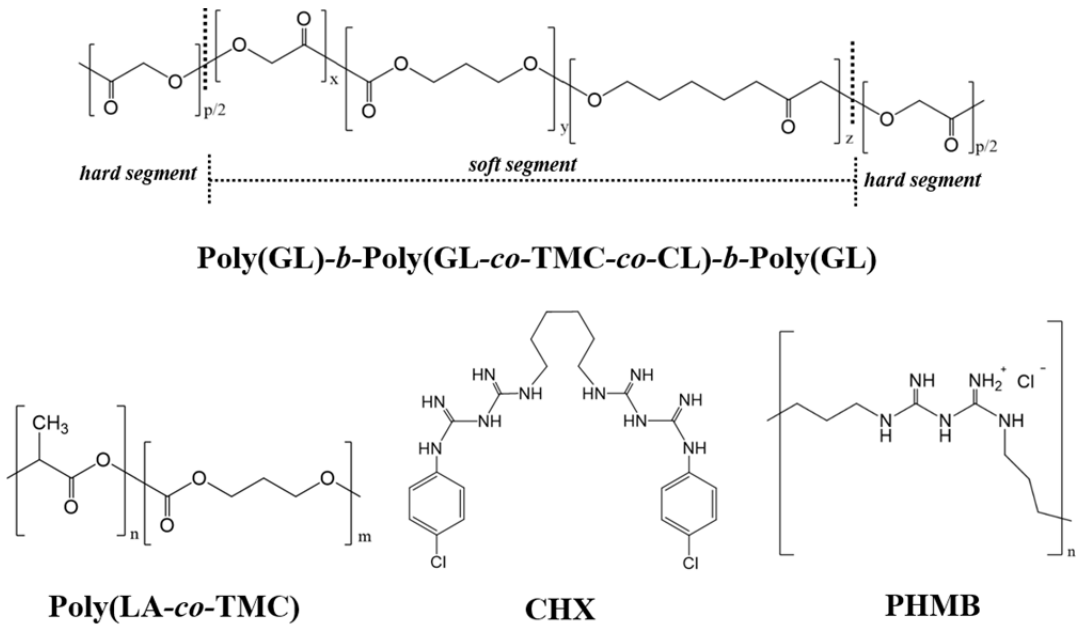

Figure 1. Chemical structures of poly(GL)-*b*-poly(GL-*co*-TMC-*co*-CL)-*b*-poly(GL) (Monosyn^{TM}), the coating poly(LA-co-TMC) copolymer and the selected CHX and PHMB bactericides.

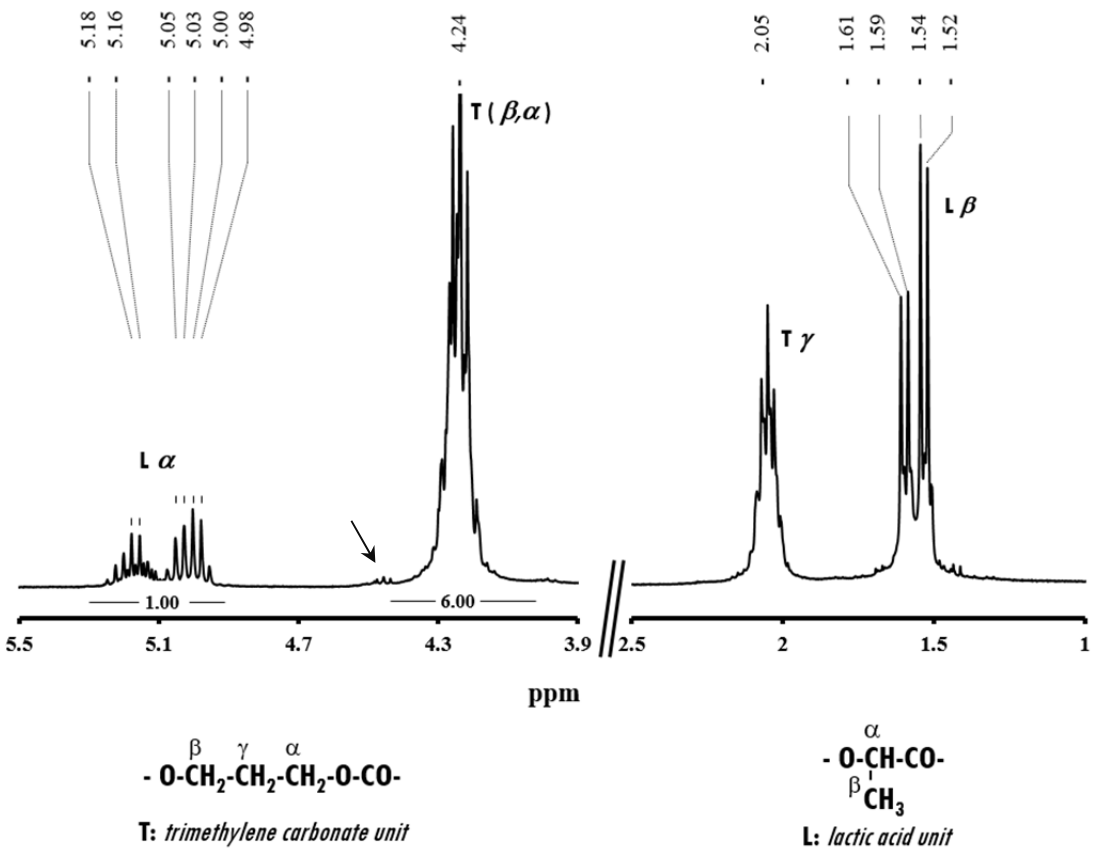

Figure 2. ^{1}H NMR spectrum of the coating copolymer with indication of peaks associated with trimethylene carbonate (T) and acid lactic (L) units as labeled in the chemical formula. Small arrow points to the presence of a minor amount of trimethylene carbonate monomer for samples taken at a reaction time slightly shorter than that corresponding to a complete conversion.

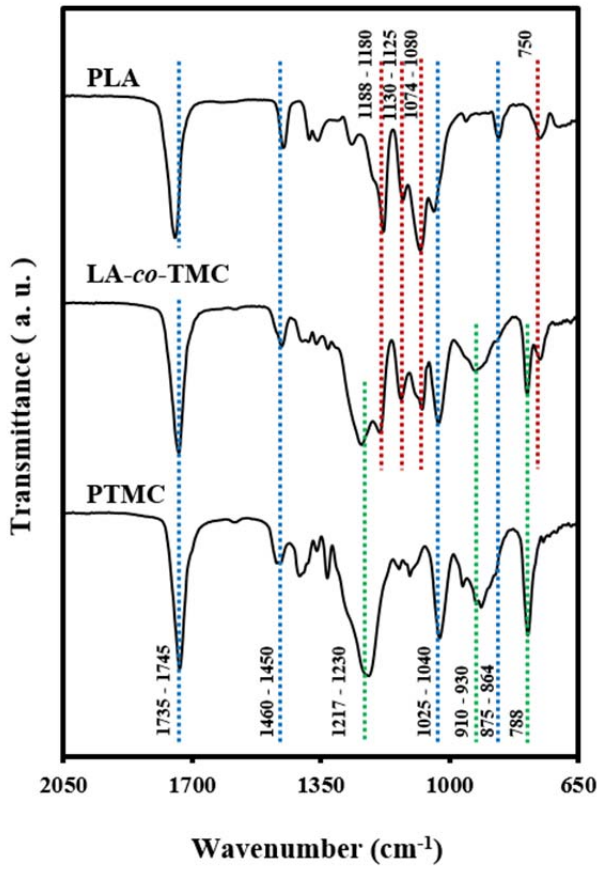

Figure 3. FTIR spectra (2050-650 cm^{-1}) of PLA, PTMC and the synthesized copolymer. Characteristic peaks of PLA and PTMC are indicated by red and green dashed lines, respectively, whereas common peaks are indicated by the blue dashed lines.

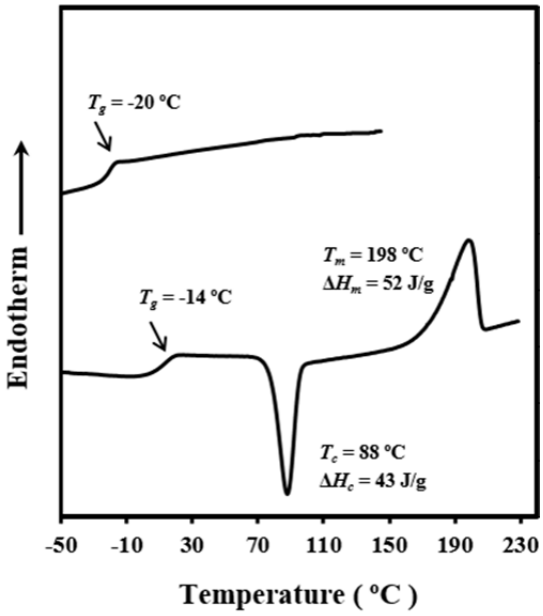

Figure 4. DSC heating traces of poly(GL)-*b*-poly(GL-*co*-TMC-*co*-CL)-*b*-poly(GL) (down) and the coating copolymer (up).

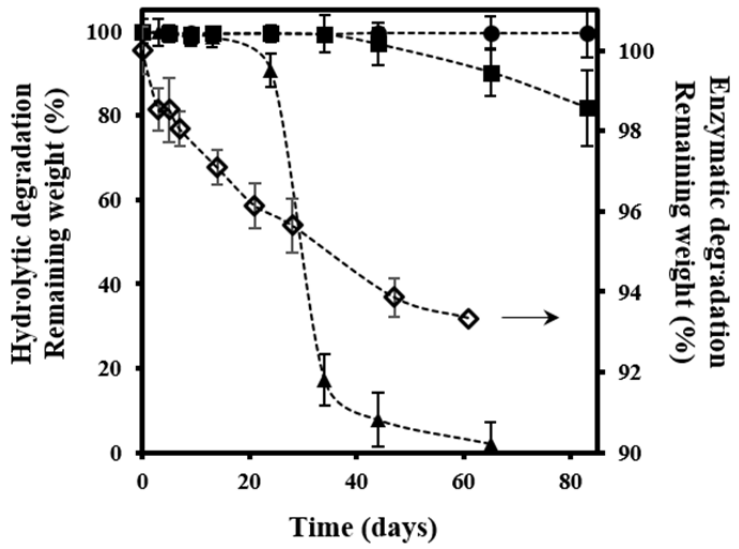

Figure 5. Remaining weight percentage of poly(LA-*co*-TMC) coating sample exposed to a pH 7.4 hydrolytic degradation medium at 70 ºC (▲), 50 ºC (■) and 37 ºC (●) and a porcine pancreatic lipase enzymatic medium (◊).

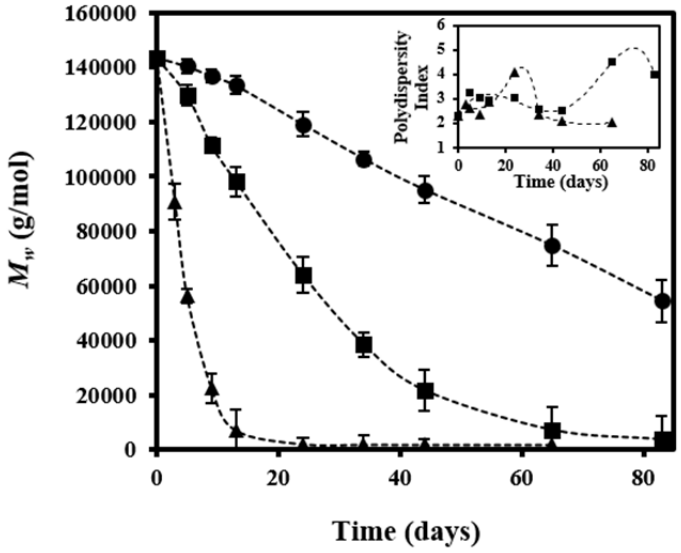

Figure 6. Changes in the weight average molecular weight of poly(LA-*co*-TMC) coating sample exposed to a pH 7 hydrolytic degradation medium at 70 ºC (▲), 50 ºC (■) and 37 ºC (●). Changes in the polydispersity index during accelerated degradation are shown in the inset.

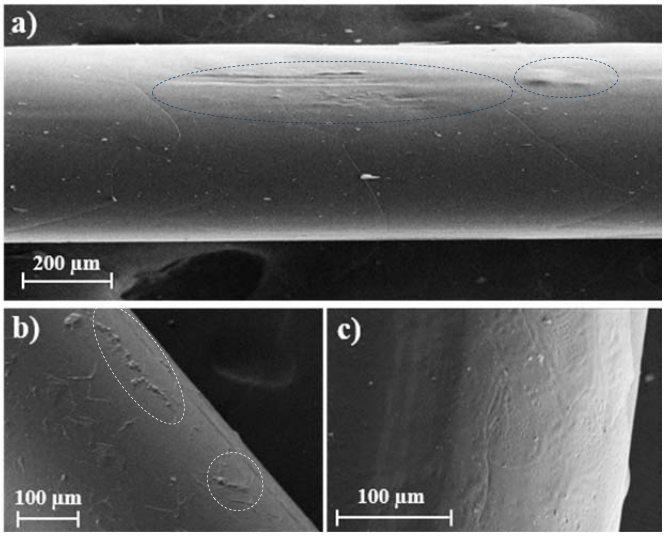

Figure 7. Scanning electron micrographs of a monofilament of the poly(GL)-*b*-poly(GL-*co*-TMC-*co*-CL)-*b*-poly(GL) suture with the following treatments: a) coating by immersion for 5 s in an ethyl acetate bath containing 10 *w*/*v*-% of poly(LA-*co*-TMC), b) immersion in a methanol bath containing 3 *w*/*v*-% of PHMB and c) a first immersion in a methanol bath containing 3 *w*/*v*-% of PHMB and then in an ethyl acetate bath containing 3 *w*/*v*-% of poly(LA-*co*-TMC) (c).

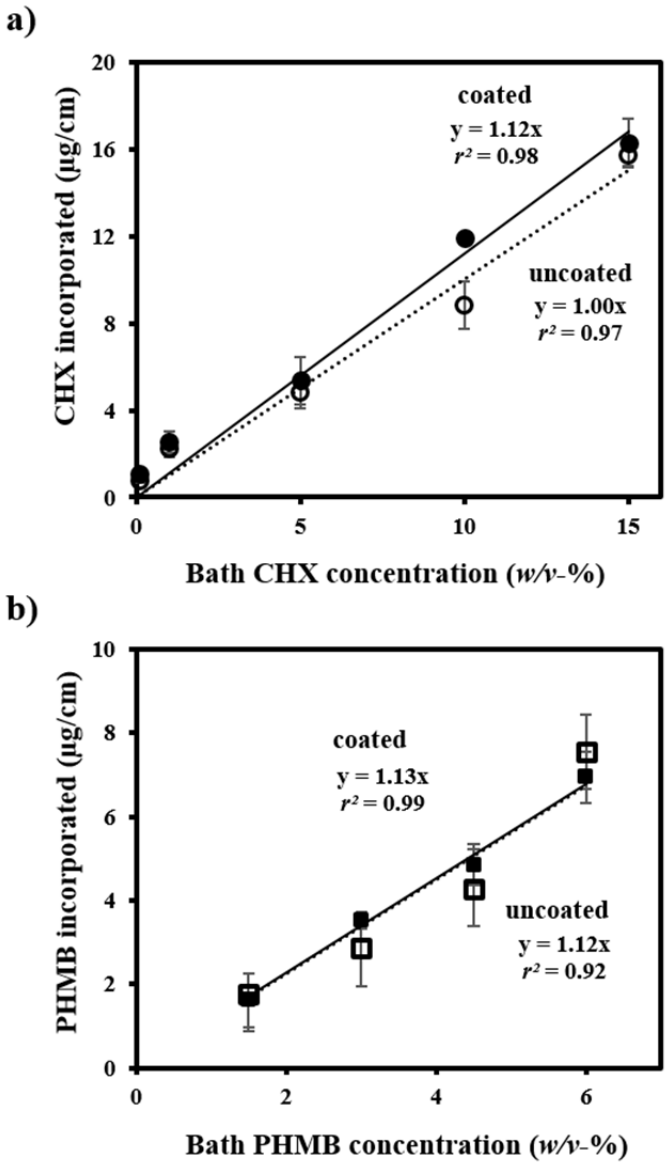

Figure 8. Plot of the amount of chlorhexidine (●) and PHMB (■) incorporated into the poly(GL)-*b*-poly(GL-*co*-TMC-*co*-CL)-*b*-poly(GL) suture (drug weight/suture length) versus drug concentration of ethanol and methanol baths. Results are given for solutions with (solid lines) and without (dashed lines) poly(LA-*co*-TMC).

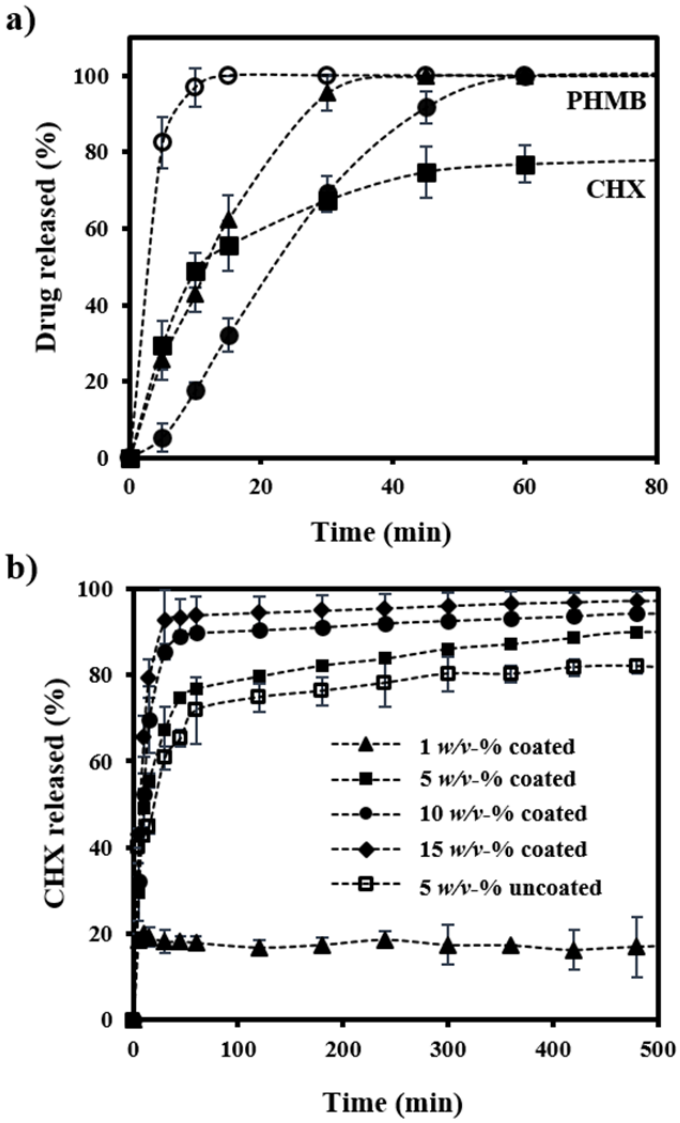

Figure 9. a) PHMB release percentages in PBS-EtOH 30:70 medium for uncoated (○) and coated (●) sutures. For the sake of completeness, data for an EtOH medium are also plotted (▲) for the coated suture as well as the CHX release percentage plot in PBS-EtOH 30:70 medium for the coated suture (■). Samples were obtained from baths containing 6 *w*/*v*-% and 5 *w*/*v*-% of PHMB and CHX, respectively. b) CHX release percentages in a PBS-EtOH 30:70 medium for coated sutures loaded in baths with 15 *w*/*v*-% (♦),10 *w*/*v*-% (●), 5 *w*/*v*-% (■) and 1 *w*/*v*-% (▲) of CHX. For the sake of completeness, data for an uncoated suture coming from a bath containing 5 *w*/*v*-% (□) of CHX are also plotted.

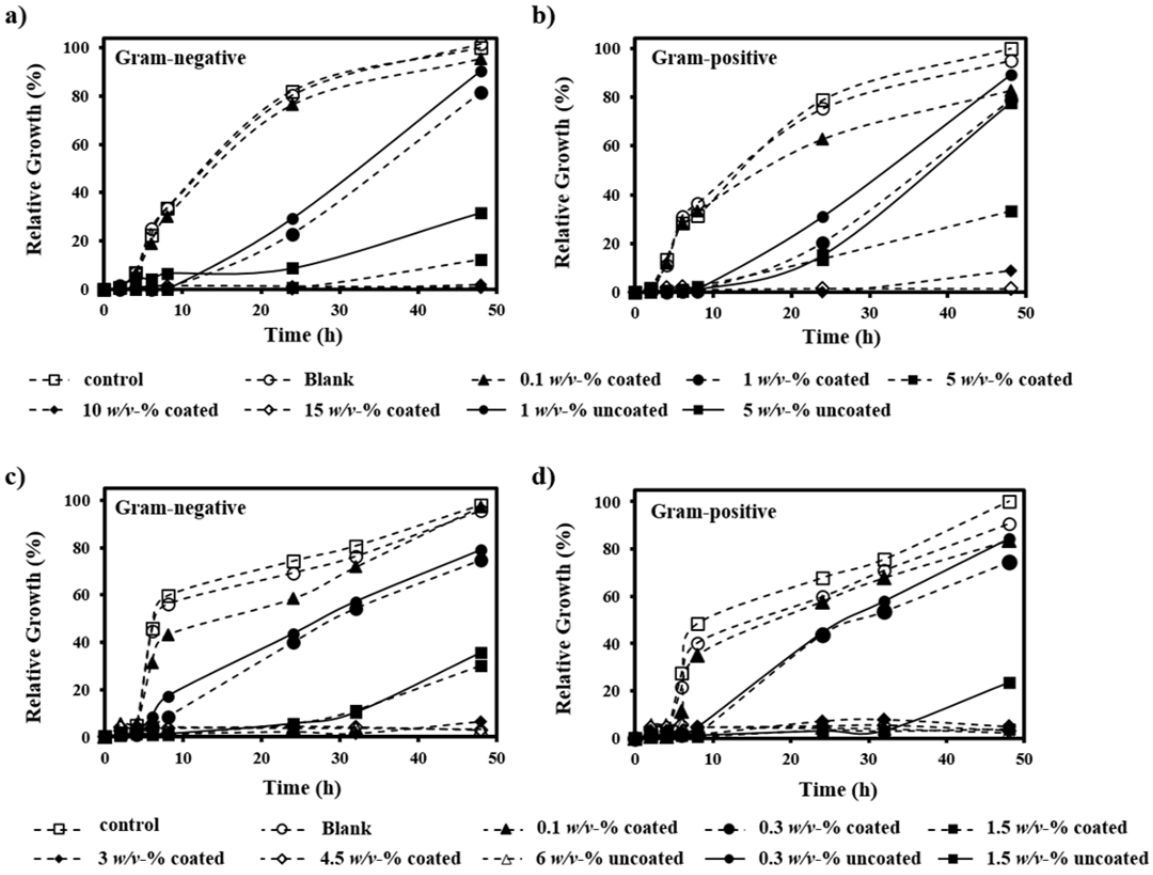

Figure 10. Growth curves of *E. coli* (a,c) and *S. epidermidis* (b,d) on culture plate as positive control (□), coated suture as blank (○) and poly(LA-*co*-TMC) coated sutures (dashed lines) loaded in baths with the indicated *w*/*v*-% of CHX (a,b) and PHMB (c,d). For the sake of completeness, data for uncoated sutures loaded from selected baths are also plotted (solid lines).

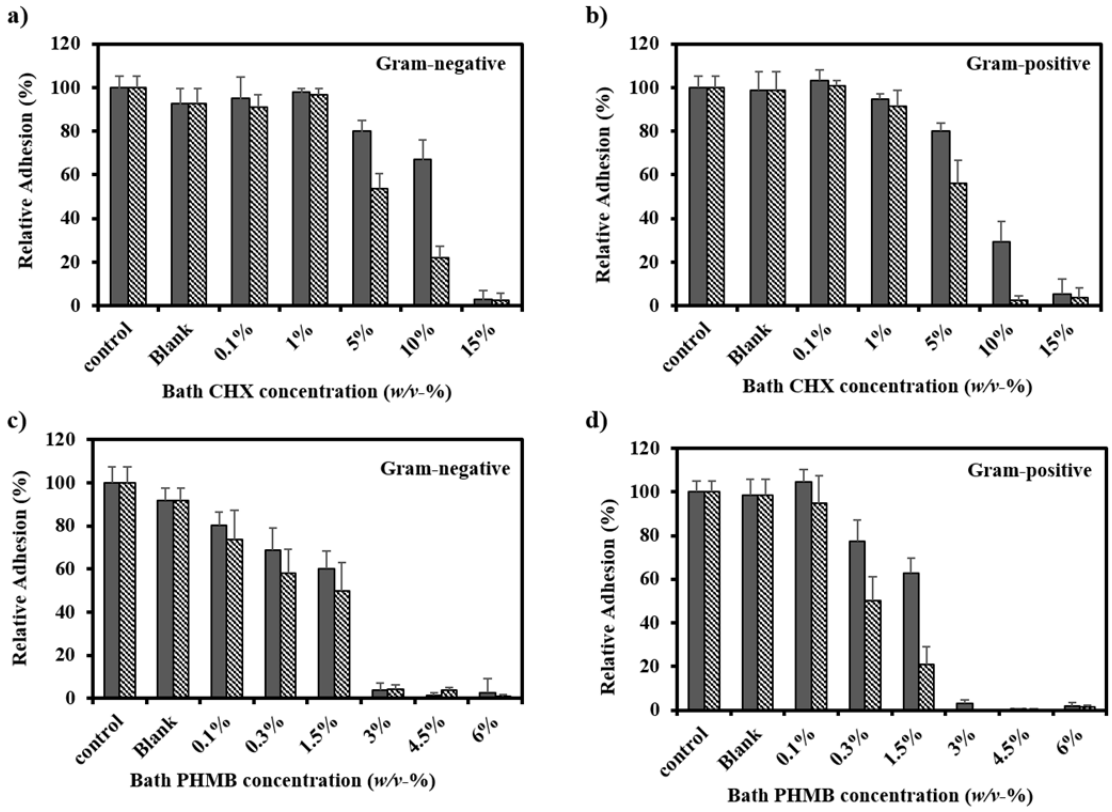

Figure 11. Adhesion of *E. coli* (a,c), and *S. epidermidis* (b,d) bacteria on uncoated (gray bars) and poly(LA-*co*-TMC) coated (grid bars) sutures loaded in baths with the indicated concentrations of CHX (a,b) and PHMB (c,d). Data concerning the culture plate as positive control and the coated and uncoated sutures as blank are also provided.

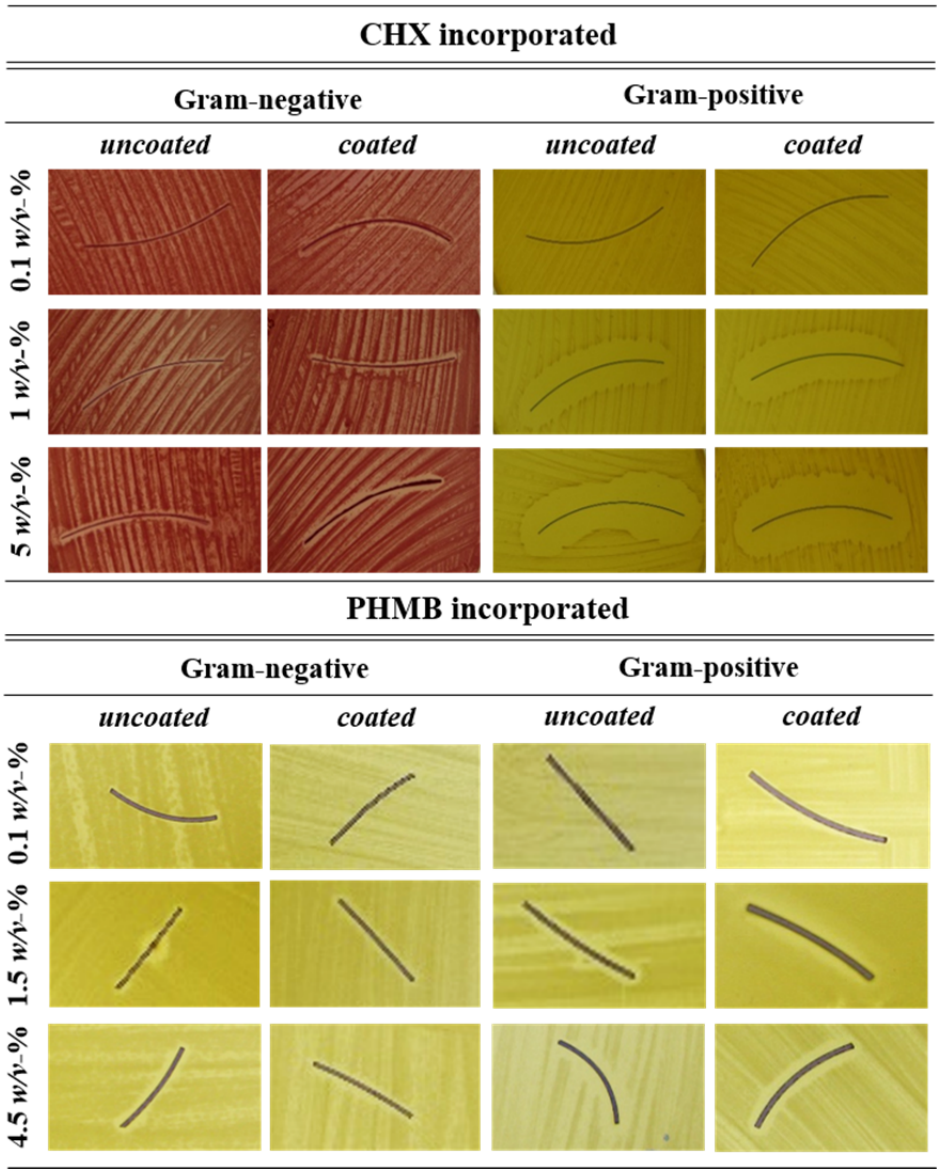

Figure 12. Agar tests showing the inhibition zone of *E. coli* and *S. epidermidis* bacteria caused by uncoated and poly(LA-*co*-TMC) coated sutures loaded in baths with the indicated CHX and PHMB concentrations.

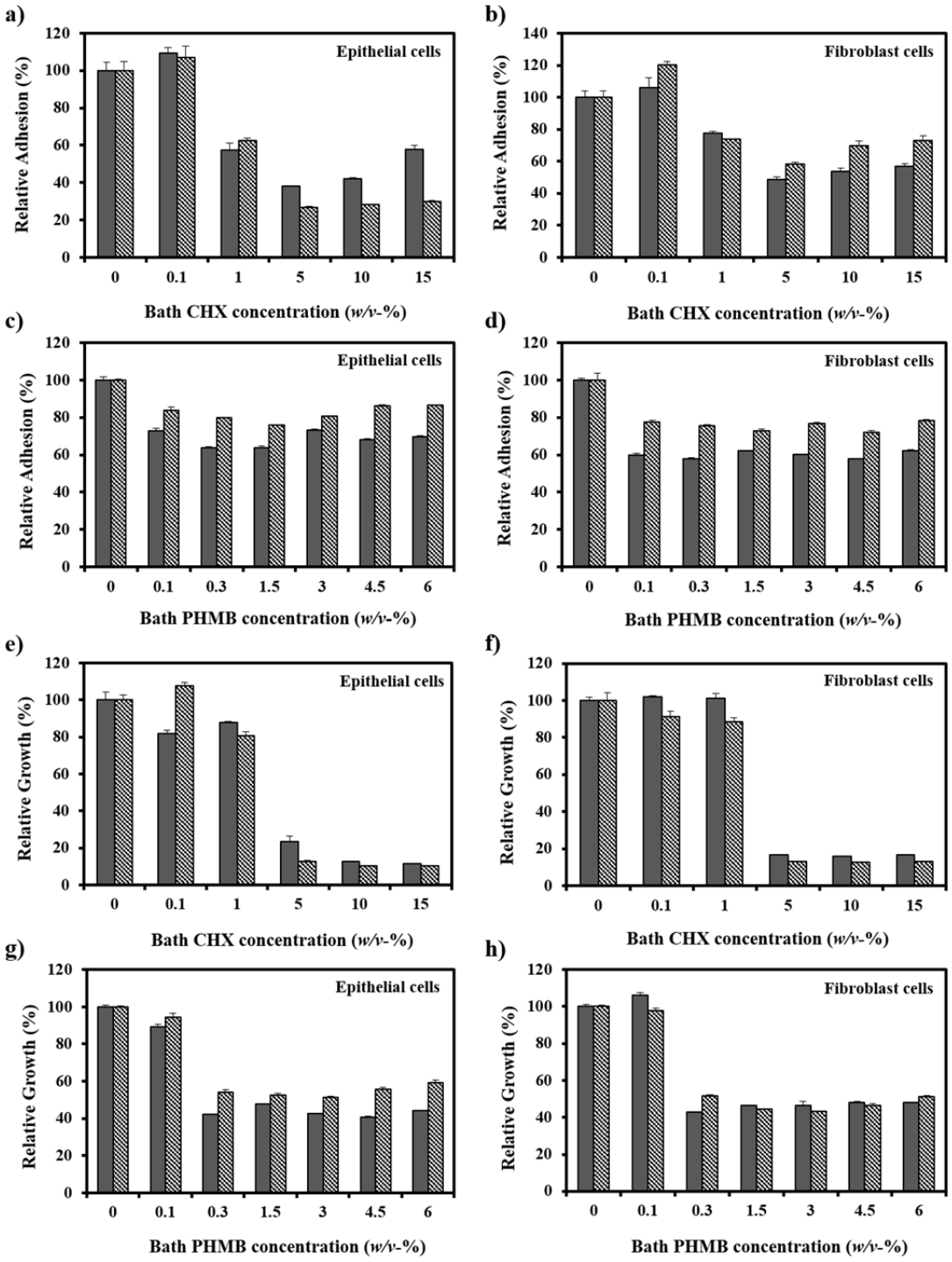

Figure 13. Adhesion (a-d) and proliferation (e-h) of Vero (a,c,e,g) and COS-7 (b,d,f,h) cells on uncoated (gray bars) and poly(LA-*co*-TMC) (grid bars) coated sutures loaded in baths with the indicated concentrations of CHX (a,b,e,f) and PHMB (c,d,g,h). Data concerning the culture plate as positive control are also provided.

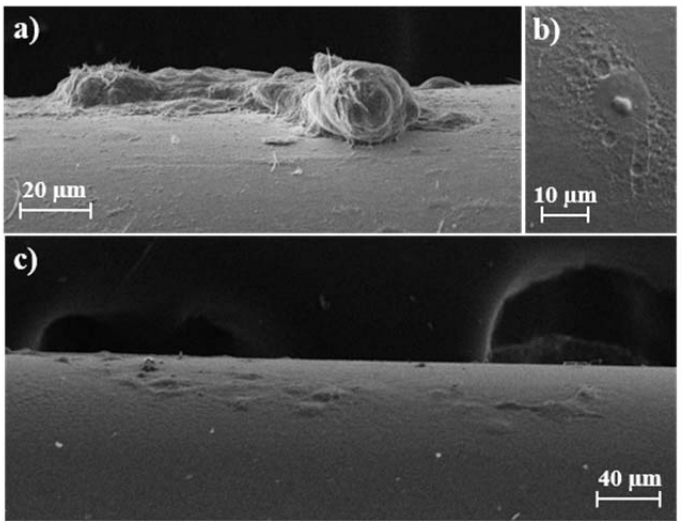

Figure 14. SEM micrographs of Vero (a,b) and COS-7 (c) cell growth on poly(LA-*co*-TMC) coated sutures loaded in baths with CHX (a,b) and PHMB (c) concentrations of 1 *w*/*v*-% and 1.5 *w*/*v*-%, respectively.